



Andrew Lees and Peter Matthias, Tensar International

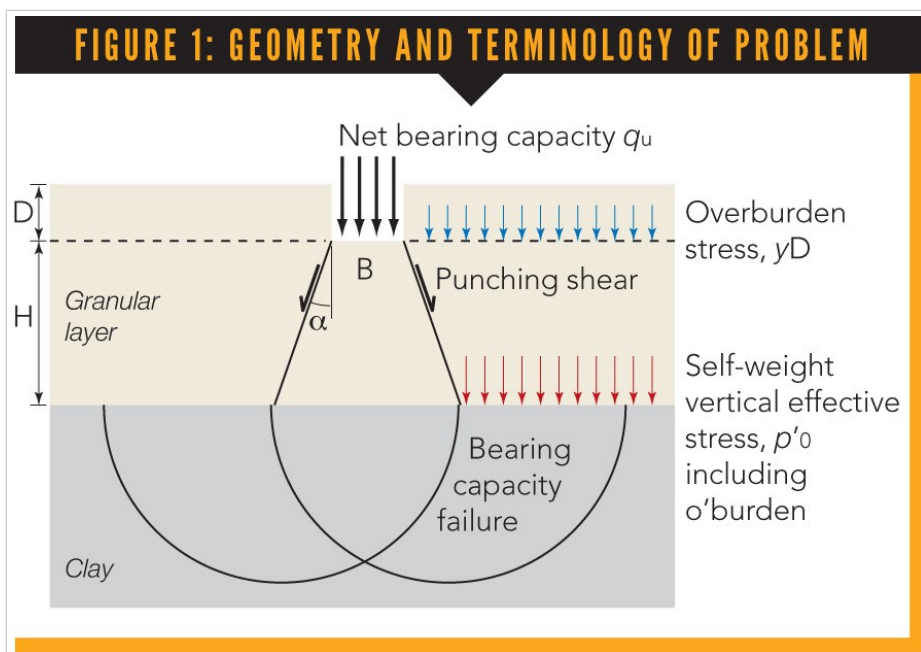
## Notation

$B$	Foundation width or diameter
$D$	Foundation embedment depth
$H$	Granular layer thickness between foundation base and clay
$L$	Foundation length
$T$	Granular layer load transfer efficiency
$p'_0$	Effective vertical stress at base of granular layer
$q_g$	Net bearing capacity of granular layer of infinite depth
$q_s$	Surface bearing capacity of clay
$q_u$	Net bearing capacity of granular layer on clay
$s_u$	Undrained shear strength of clay
$\alpha$	Load spread angle
$\gamma$	Weight density of granular layer
$\varphi'$	Internal friction angle of granular layer

## Introduction

Granular layers are often used in working platforms and beneath foundations to improve load spread and bearing capacity on weaker clay soils. The installation of a stiff polymer mesh (geogrid) within the granular layer can improve the bearing capacity significantly, allowing thinner granular layers to be installed and bringing cost savings associated with the smaller volumes of material.

Bearing capacity failure involves punching shear through the granular layer and a bearing capacity mechanism in the underlying clay (figure 1), unless the granular layer exceeds a critical thickness above which shear failure occurs entirely within the upper layer. Existing design methods (without geogrid) include the semi-empirical Meyerhof (1974) or Hannah and Meyerhof (1980) method and the load spread or projected area method. The former is generally more accurate and is recommended by BRE (2004) for the routine design of piling platforms but suffers from the drawback that punching shear coefficients were derived empirically from model footing tests at 1g and not in a non-dimensional form so are appropriate only for the granular layer density and thickness used in the derivation (Burd and Frydman, 1997).



In the load spread method, the granular layer is assumed to spread load uniformly to the underlying clay and the shear strength contribution of the granular layer is ignored (Terzaghi and Peck, 1948; Yamaguchi, 1963). The angle  $\alpha$  of load spread to the vertical is assumed the same as the angle of the straight shear planes in the granular layer. Many values have been proposed, as summarised by Craig and Chua (1990), and the main drawback of this method is the difficulty of determining  $\alpha$ . Brocklehurst (1993) and Ballard et al (2011) showed that  $\alpha$  is also influenced by the shear strength of both the granular layer and the underlying clay.

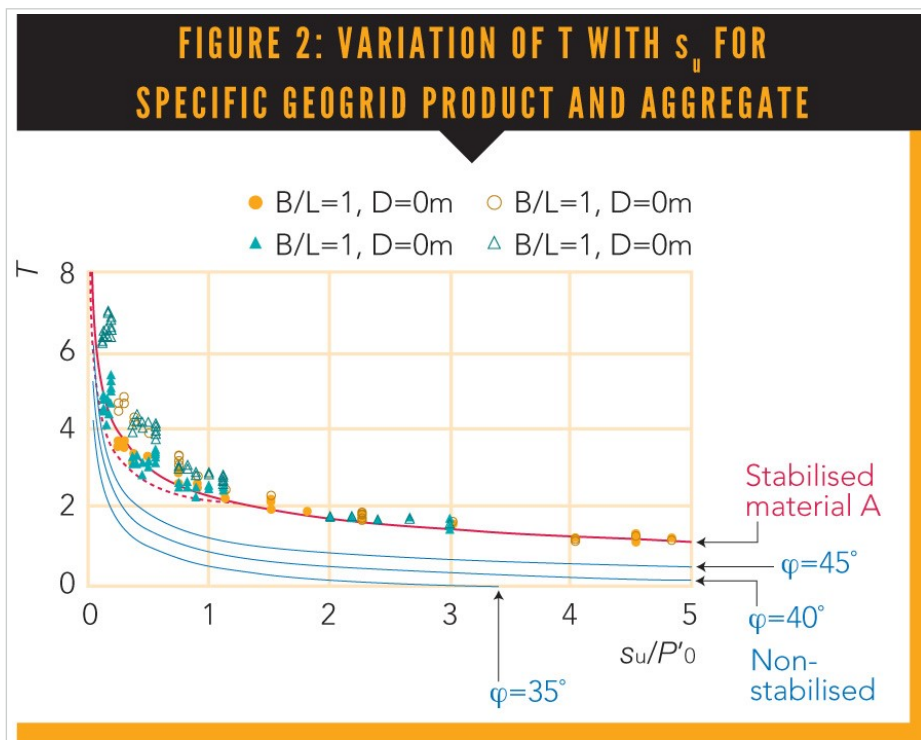
Lees (2019) derived a non-dimensional relationship (equations 1 and 2) between bearing capacity ratio  $q_u/q_s$  and the load transfer efficiency of the granular layer expressed as a dimensionless  $T$  value.

$$\frac{q_u}{q_s} = 1 + T \frac{H}{B} \leq \frac{q_g}{q_s} \quad (\text{strip footing}) \quad (1)$$



$$\frac{q_u}{q_s} = \left(1 + T \frac{H}{B}\right)^2 \leq \frac{q_g}{q_s} \quad (\text{square or circular footing}) \quad (2)$$

The T value depends on the shear strengths of the two layers and is derived by numerical analysis (eg FEA) parametric study and physical testing, the results of which are shown as the lower non-stabilised curves in figure 2. In design, this allows a simple calculation to be made of the bearing capacity directly from the shear strengths of the individual soil layers without the need for empirical-based charts. It can be applied to both surface and shallow embedded foundations, circular and rectangular and with dry or saturated granular layers. The bearing capacity of foundations with B/L ratios between 0 and 1 can be determined by linear interpolation. The inequalities in equations 1 and 2 are needed to check for cases where shear failure entirely within the granular layer is critical.



This paper addresses this drawback by presenting a modification to the new “T-Value Method” (Lees, 2019) to include the benefit of installing multi-axial stabilising geogrid in a granular layer overlying clay on its bearing capacity. The dependency of the stabilisation benefit on geometrical parameters and  $s_u$  will be determined by FEA validated by full-scale testing.

The Meyerhof (1974) and load spread methods have both been modified to include the benefit of installing geogrid within the granular layer. A simple modification to the former was proposed in BRE (2004) involving the addition of a factored geogrid tensile strength to the design equation while Milligan et al (1989a and b) added the geogrid benefit to the load spread method by taking account of additional shear stresses generated at the interface between the granular layer and clay, limited by the tensile strength of the geogrid. These methods are intended for reinforcing geogrid where geogrid performance is defined in terms of a tensile strength obtained by testing in air. They are not suited to multi-axial geogrid that is designed primarily to stabilise the aggregate rather than provide tensile reinforcement. BRE (2011) recognised that alternative design methods may be used for geosynthetics in situations

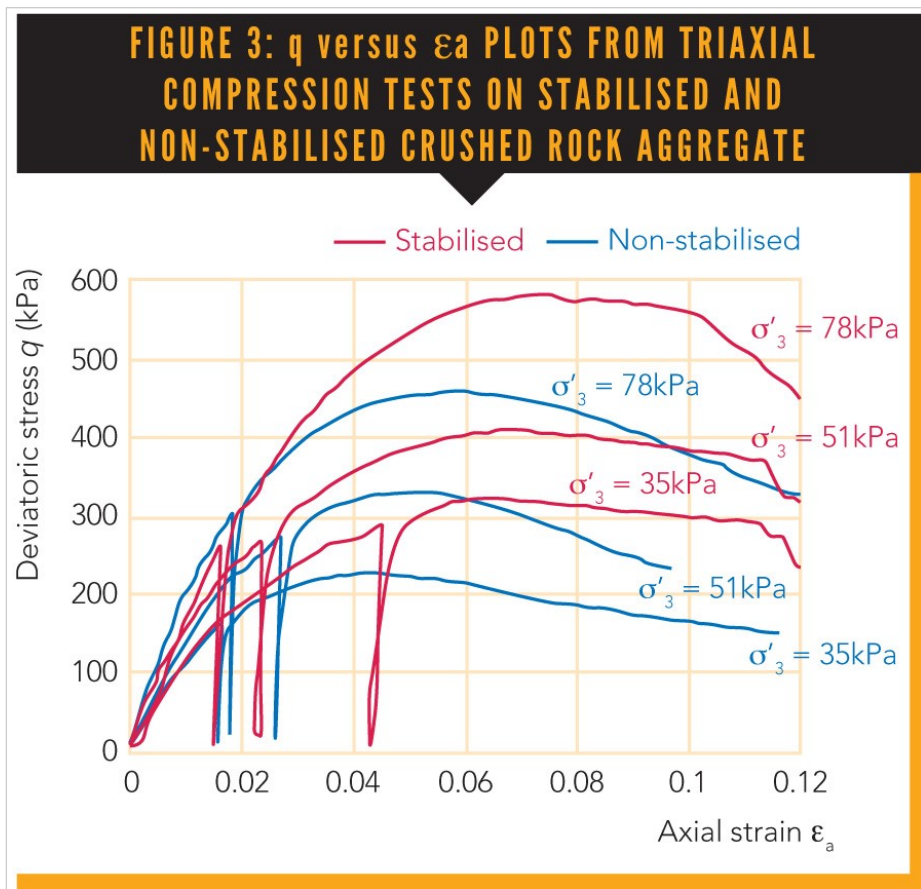


for which they have been validated. The benefit of stabilising geogrid on bearing capacity has been defined for proprietary design methods in terms of an enhanced load spread angle validated by field experience and laboratory and full-scale testing. The drawback with this method has been the inability to demonstrate analytically the benefit of geogrid stabilisation.

### Stabilised soil behaviour

Stiff, punched and drawn multi-axial (triangular aperture) polypropylene (PP) geogrid was designed primarily to restrict the movement of soil particles in and around its apertures – a function defined as stabilisation in the International Geosynthetic Society’s latest guide (IGS, 2018) – and there is evidence (eg Bussert and Cavanaugh, 2010) that the stabilising effect of geogrid extends a significant distance from the geogrid plane, typically 300mm or more.

Lees and Clausen (2019) performed large triaxial compression tests (specimen size 0.5m diameter x 1m height) with vacuum-applied confining stress on a dry, crushed diabase rock with and without a stiff, punched and drawn multi-axial PP geogrid placed at mid-height. The crushed rock had a coefficient of uniformity  $C_u$  of 23 with  $D_{60} = 8\text{mm}$  and  $D_{100} = 40\text{mm}$ . It was compacted to at least 95% maximum dry density. The plots of averaged deviatoric stress  $q$  against averaged axial strain  $\epsilon_a$  at three different confining stresses with and without the geogrid in figure 3 show an enhanced peak shear strength in the geogrid-stabilised soil at all three confining stresses. These formed a markedly non-linear failure envelope in the stabilised case due to restraint on particle translation and rotation, significantly increasing the work done required to shear and dilate the specimen.

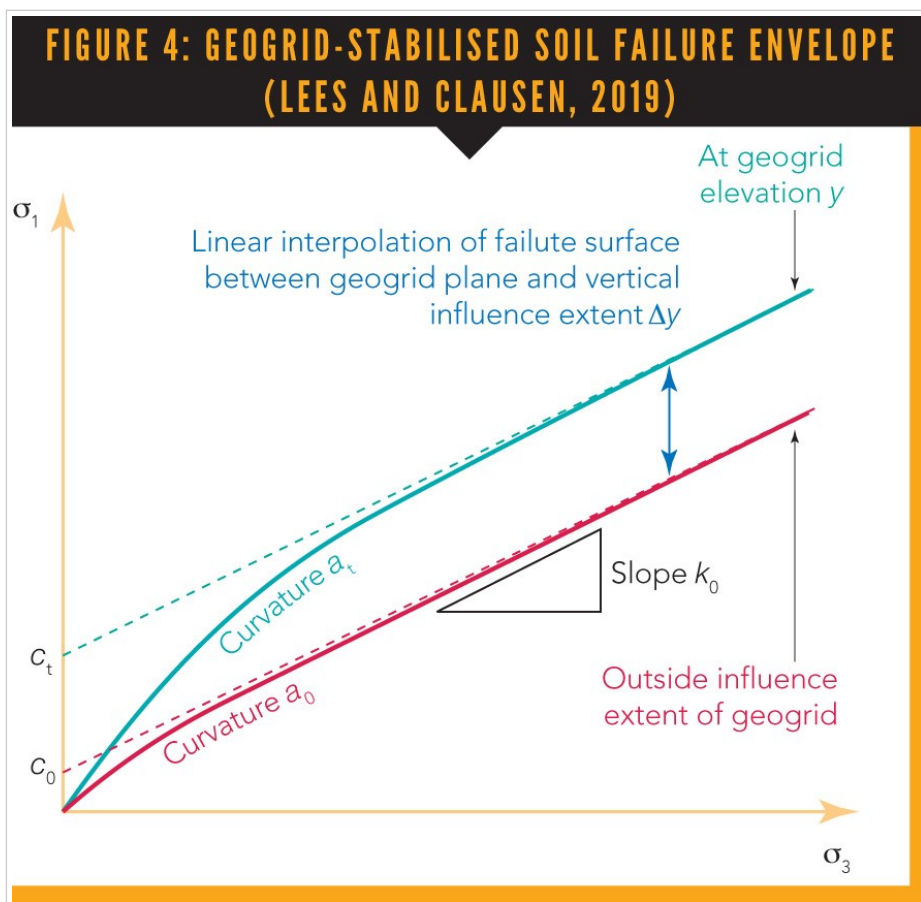


Also of note is the larger strains required to cause significant softening of the stabilised granular soil compared with the non-stabilised. Peak failure occurred at axial strains of about 4 to 5% in the non-stabilised case after which dilation-induced softening occurred whereas



the stabilised specimens experienced significant softening at more than about 10% axial strain. Strain levels at the onset of bearing capacity failure in clays are generally up to about 10% depending on the clay stiffness, meaning that lower post-peak shear strengths are appropriate for overlying non-stabilised granular layers when calculating bearing capacity for design but, in many more cases, it would be appropriate to adopt the peak strength of stabilised granular layers due to the higher strain level at which significant strength softening occurs.

Since the restraint on soil particles would be at a maximum at the geogrid plane and reduce with distance from the plane, the failure envelope was considered to vary (assumed linearly) from a maximum at the geogrid plane to the non-stabilised failure envelope at a perpendicular distance  $\Delta y$ , beyond which the non-stabilised failure envelope prevailed, as illustrated in figure 4. The non-stabilised failure envelope can be obtained straightforwardly from shear strength tests on the granular material without geogrid and the maximum failure envelope and  $\Delta y$  determined from the back analysis of shear strength tests with one or more layers of the specific geogrid product being tested.



A linear elastic perfectly-plastic (LEPP) constitutive model called the Tensar Stabilised Soil Model (TSSM) with the non-linear failure envelope was implemented into the Plaxis 2D 2018 (Brinkgreve et al, 2018) FEA software and found to provide accurate predictions of failure stress in back-analyses of the triaxial compression tests (Lees and Clausen, 2019).

### FEA parametric study

The parametric study of bearing capacity was performed by two-dimensional FEA using Plaxis 2D 2018 in plane strain for strip loads and axisymmetry for equivalent square loads. The TSSM was used for the granular material described in the previous section with a specific stabilising



punched and drawn PP multi-axial geogrid denoted together as “stabilised material A” with the input parameters shown in table 1. The clay was modelled with an LEPP model with Tresca failure criterion with undrained Young’s modulus  $E_u$  taken as  $800s_u$  and Poisson’s ratio  $\nu_u$  as 0.495. Geometrical and clay shear strength parameters were varied as shown in table 2 (the square footing  $B$  values give the same foundation area as the circular footing simulated in FEA). In all cases, one geogrid plane was placed at the base of the granular layer. When  $H$  was 0.45m and 0.6m, an additional geogrid plane was placed 0.3m above the base of the granular layer, and when  $H$  was 0.75m and 0.9m, a third geogrid plane was placed at 0.6m above the base of the granular layer. A rigid, rough footing was assumed in all cases and displacement control was used to increase the load to failure.

**TABLE 1: TSSM INPUT PARAMETERS FOR STABILISED MATERIAL A**

Parameter	Value
$k$	5.7
$c_0$	56kPa
$a_0$	2.0
$m$	5.7
$b$	2.0
$\Delta_y$	0.30m
$c_t$	350kPa
$a_t$	14
$E$	50MPa
$\nu$	0.25
$\gamma$	21kN/m <sup>3</sup>

**TABLE 2: INPUT PARAMETERS VARIED IN THE FEA PARAMETRIC STUDY**

$s_u$ (kPa)	5, 15, 30, 80
B/L	0 (plane strain), 1 (axisymmetric)
B (m)	0.3, 0.6, 0.9, 1.2, 1.8, 2.4
H (m)	0.3, 0.45, 0.6, 0.75, 0.9
$\gamma D$ (kPa)	0, 20

The output from the parametric study is presented in figure 2 in terms of the T value back-calculated using equations 1 and 2 from output of  $q_u$  and adopting  $N_c = 5.14$  and 6.2 for  $q_s$  in the plane strain and axisymmetric cases respectively. All cases, including with overburden stress ( $\gamma D > 0$ ), are shown to follow a similar trend when  $s_u$  is normalised by  $p'_0$ . The line



shown is considered a best fit line for the plane strain ( $B/L=0$ ) cases and a lower bound for the axisymmetric cases ( $B/L=1$ ) and follows equation 3 and can be applied for granular materials of similar characteristics with the specific geogrid product tested. The interactions between aggregates and geogrid are highly complex so similar products may not follow this relationship and should be derived specifically for each product following the same procedure with full-scale validation.

$$T = 2.9 \left( \frac{s_u}{p'_0} \right)^{-0.32} - 0.6 \quad (3)$$

The line follows a similar trend to those derived for non-stabilised granular layers with different  $\varphi'$  angles shown where the T value increases with the  $\varphi'$  value. The higher T value obtained with a stabilised granular layer is consistent with the higher shear strength imparted to the soil by the stabilising geogrid. The higher ductility of the stabilised granular layer also allows the peak strength to be used in design whereas for non-stabilised soil the strain levels at bearing capacity failure typically exceed peak failure strains in dense granular materials and post-peak shear strengths should be used in design.

The outputs of T value become increasingly sensitive to  $s_u/p'_0$  as  $s_u/p'_0$  values fall below about 1.25 since stress changes have a proportionally bigger effect on bearing capacity as shear strength becomes very low. At  $s_u/p'_0$  values below 1.25, it is recommended to apply the correction shown in equation 4 to the T value to take account of this uncertainty. This correction plots as the dashed line in figure 2 which forms a lower bound to all the values obtained in the FEA parametric study. Alternatively, more advanced analysis (eg FEA) than the T-value method could be undertaken for bearing capacity calculations in very soft clays.

$$T_{corr} = \frac{T}{1 + 0.2 (1.25 - s_u/p'_0)} \quad \text{when } s_u/p'_0 < 1.25 \quad (4)$$

## Validation

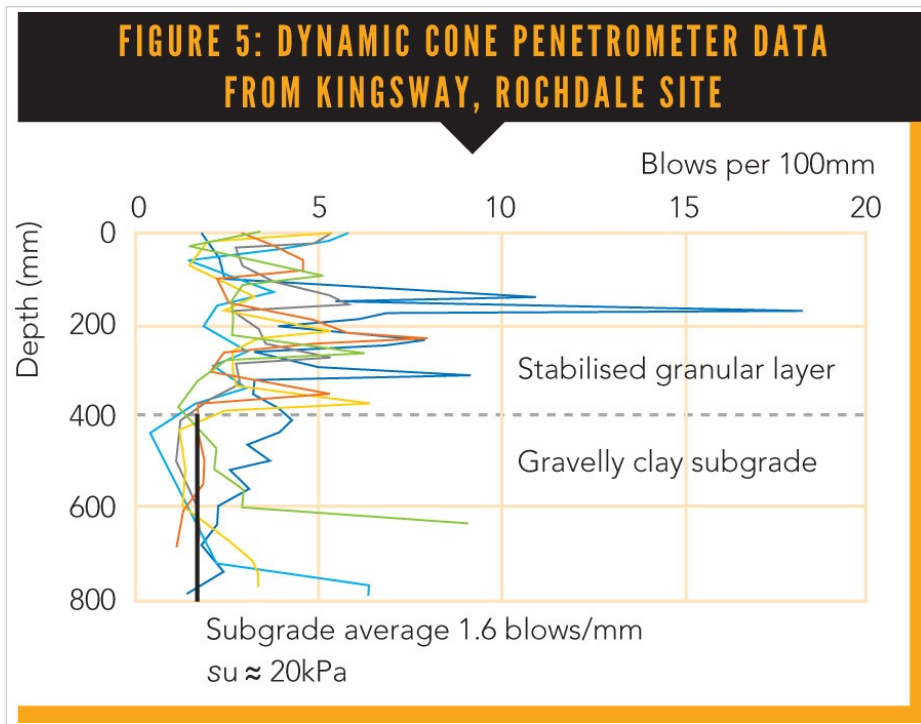
The stabilisation function of geogrid and enhanced shear strength are heavily dependent on the interactions between geogrid components and the aggregate particles that are being restrained. As such, the T-value to subgrade strength relationship should be derived for specific geogrid products and aggregate types and then validated by full-scale testing appropriate for the foundation or track width to be supported. An example of an appropriate full-scale validation test is presented in this section.

A 0.4 m thick platform of the same characteristics as “stabilised material A” including one layer of the multi-axial stabilising geogrid at its base was laid and compacted over the existing ground during construction of the Kingsway Business Park in Rochdale, Greater Manchester in December 2018. The existing ground was a reworked Made Ground comprised of a firm gravelly clay to about 4m depth.

Five plate load tests (PLT) on the platform surface were undertaken in accordance with BS 1377-4 Clause 4.1 (BSI, 1990). A large 600mm diameter plate was used for the tests to match the expected loaded width on the platform and to ensure that the critical failure mechanism

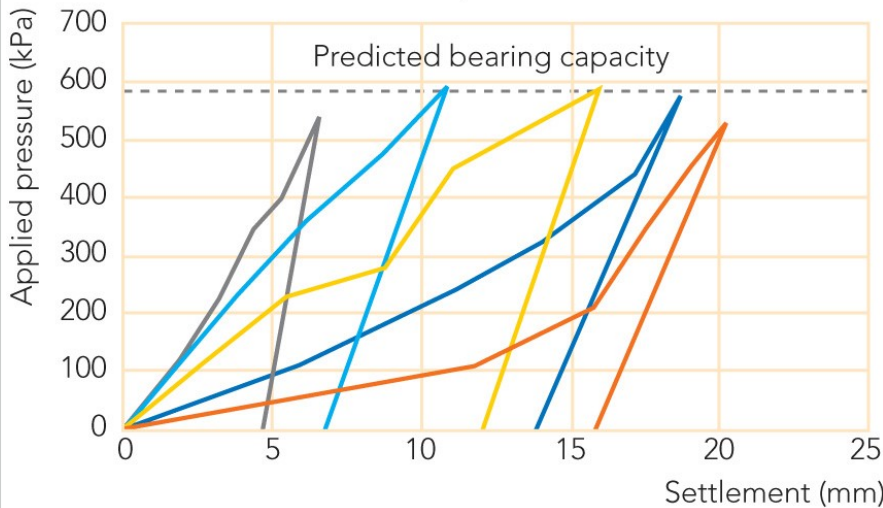


was punching shear through to the subgrade rather than shear failure entirely within the granular layer. Dynamic cone penetrometer (DCP) testing was also undertaken in accordance with Jones (2004) at each PLT location to confirm the platform thickness and to determine the  $s_u$  value of the subgrade. Since  $s_u$  is related to moisture content and varies, it is important to take measurements on the same day as the PLTs and the simple, lightweight nature of the DCP allows this on a live construction site. However, correlations between blow count and  $s_u$  are approximate, especially for soft, fine-grained materials and results are subject to rod alignment and skin friction as well as operator error. The results of the DCP testing are presented in figure 5 as blows per 100mm penetration where the 0.4m thick platform is apparent. An average value for the subgrade is shown for which an  $s_u$  value of 20kPa was derived using Look (2014).



The bearing capacity of a 600mm diameter plate on a 0.4m thick platform of Stabilised Material A on a subgrade of  $s_u = 20\text{kPa}$  was calculated as 585kPa using the method presented in this paper. The PLT results are plotted in figure 6 where it is shown that the bearing pressure reached the approximate calculated bearing capacity on all five occasions without any indication of bearing failure visible on site or apparent in the load-deflection data. The load could not be increased further in an attempt to measure the fully mobilised bearing capacity because the safe capacity of the test equipment had been reached. Nevertheless, the actual bearing capacity exceeded the calculated value which provided useful validation of the proposed design method.

**FIGURE 6: PLATE LOAD TEST DATA FROM KINGSWAY, ROCHDALE SITE**



**Example**

A worked example is presented in this section as shown in table 3 for a working platform with track loading. Note that the parameters are appropriate only for a working platform composed of a granular material and stabilising geogrid product of the same characteristics tested in triaxial compression to obtain the parametric study outputs and which have subsequently been validated by full-scale testing as described earlier in this paper.

**TABLE 3: CALCULATION EXAMPLE FOR WORKING PLATFORM**

**Example:** Track loading on stabilised working platform with the same characteristics as those in the parametric study described earlier in this paper.

**Input data:**

$B = 0.6m, L = 3.0m, s_u = 40kPa, \gamma = 18kN/m^3, H = 0.3m$

$p'0 = 0.3 \times 18 = 5.4kPa$

$s/p'0 = 40/5.4 = 7.4$

$T = 0.93$  (from Equation 3)

**B/L = 1:**

$q_t = s_u N_s = 1.2 \times 5.14 \times 40 = 246.7kPa$

**Equation 2:**  $q_u/q_t = (1 + TH/B)^2 = (1 + 0.93(0.3/0.6))^2 = 2.15$

$q_u = 246.7 \times 2.15 = 529.5kPa$

**B/L = 0:**

$q_t = s_u N_s = 1.0 \times 5.14 \times 40 = 205. kPa$

**Equation 1:**  $q_u/q_t = (1 + TH/B) = (1 + 0.93(0.3/0.6)) = 1.46$

$q_u = 205.6 \times 1.46 = 301.2kPa$

$B/L = 0.6/3.0 = 0.2$

Interpolation between  $B/L = 1$  and  $0$ :  $q_u = 346.9kPa$

$q_u = \gamma DN_s + 1/2 B \gamma N_s = 0 + 0.5 \times 0.6 \times 18 \times 241 \times 0.94 = 1223kPa$  (taking  $\psi = 45^\circ$  for stabilised material)

$q_u \leq q_u?$  YES.

**$q_u$  taken as 347kPa**

**Conclusions**

A parametric study using FEA of strip and circular foundations was used to derive the load transfer efficiency T of a granular layer stabilised by a multi-axial PP geogrid product overlying a clay soil of a range of  $s_u$  values. This relationship between T and  $s_u$  can be used to calculate the bearing capacity of granular layers of similar characteristics stabilised with the specific geogrid product for a wide range of geometries and clay strengths. This has been demonstrated by a worked example and validated by comparison with an example full-scale field test.

The relationship between T and  $s_u$  can be determined for other granular materials and stabilising geogrid products by 2D axisymmetric and plane strain FEA parametric studies covering the range of  $s_u$  and  $H/B$  values that will be encountered, validated by full-scale testing with the same geogrid product and aggregate characteristics. FEA input parameters



should be derived from large triaxial compression tests on the granular material at the appropriate density with the specific geogrid product.

## References

- Ballard, J-C; Delvosal, P; Yonatan, P; Holeyman, A; and Kay, S; 2011. Simplified VH equations for foundation punch-through sand into clay. *Frontiers in Offshore Geotechnics II* (ed Gourvenec and White). CRC, London: 655-660.
- BRE, 2004. BR470 Working platforms for tracked plant. BRE: Watford.
- BRE, 2011. Use of “structural geosynthetic reinforcement” – A BRE review seven years on. BRE: Watford.
- Brinkgreve, RBJ; Kumarswamy, S; Swolfs, WM; and Foria, F; 2018. Plaxis 2018. Delft.
- Brocklehurst, CJ; 1993. Finite element studies of reinforced and unreinforced two-layer soil systems, DPhil thesis, University of Oxford.
- BSI (1990) Methods for test for soils for civil engineering purposes. In-situ tests. BS 1377-9:1990. British Standards Institution, London.
- Burd, HJ; and Frydman, S; 1997. Bearing capacity of plane-strain footings on layered soils, *Canadian Geotechnical Journal* 34(2): 241-253.
- Bussert, F; and Cavanaugh, J; 2010. Recent research and future implications of the actual behaviour of geogrids in reinforced soil. ASCE Earth Retention Conference (ER2010), 1-4 August, Bellevue, Washington, 460-477.
- Craig, WH; and Chua, K; 1990. Deep penetration of spud-can foundations on sand and clay. *Géotechnique* 40(4): 541-556.
- Hannah, AM; and Meyerhof, GG; 1980. Design charts for ultimate bearing capacity of foundations on sand overlying soft clay. *Canadian Geotechnical Journal* 17(2): 300-303.
- IGS. (2018). Guide to the Specification of Geosynthetics, 5th edition. International Geosynthetics Society, Jupiter FL.
- Jones, C; (2004) Dynamic cone penetrometer test and analysis. Project Report PR/INT/277/04. Transport Research Laboratory.
- Lees, AS; (2019) The bearing capacity of a granular layer on clay. *Proceedings of the Institution of Civil Engineers – Geotechnical Engineering* <https://doi.org/10.1680/jgeen.18.00116> In press.
- Lees, AS; and Clausen, J; 2019. The strength envelope of granular soil stabilised by multi-axial geogrid in large triaxial tests. *Canadian Geotechnical Journal* <https://doi.org/10.1139/cgj-2019-0036> In press.
- Look, BG; (2014) *Handbook of Geotechnical Investigation and Design Tables*, 2nd edition. Taylor & Francis Group.
- Meyerhof, GG; 1974. Ultimate bearing capacity of footings on sand layer overlying clay. *Canadian Geotechnical Journal* 11(2): 223-229.
- Milligan, GWE; Jewell, RA; Houlsby, GT; and Burd, HJ; 1989a. A new approach to the design of unpaved roads – Part I. *Ground Engineering* 22 (April): 25-29.
- Milligan, GWE; Jewell, RA; Houlsby, GT; and Burd, HJ; 1989b. A new approach to the design of unpaved roads – Part II. *Ground Engineering* 22 (November): 37-42.
- Terzaghi, K; and Peck, RB; 1948. *Soil Mechanics in Engineering Practice*, 1st ed John Wiley and Sons, New York.
- Yamaguchi, H; 1963. Practical formula of bearing value for two layered ground. In *Proceedings of the 2nd Asian Regional Conference of Soil Mechanics and Foundation Engineering*, Tokyo: 99-105.

